

# $\beta$ -decay half-lives at finite temperatures for N=82 isotones

F. Minato<sup>1</sup> and K. Hagino<sup>2</sup>

<sup>1</sup> *Innovative Nuclear Science Research Group, Japan Atomic Energy Agency, Tokai 319-1195, Japan*

<sup>2</sup> *Department of Physics, Tohoku University, Sendai 980-8578, Japan*

(Dated: November 9, 2018)

Using the finite temperature quasi-particle random phase approximation (FTQRPA) on the basis of finite temperature Skyrme-Hartree-Fock + BCS method, we study  $\beta^-$ -decay half-lives for even-even neutron magic nuclei with N=82 in a finite temperature environment. We find that the  $\beta^-$ -decay half-life first decreases as the temperature increases for all the nuclei we study, although the thermal effect is found to be small at temperatures relevant to r-process nucleosynthesis. Our calculations indicate that the half-life begins to increase at high temperatures for open shell nuclei. We discuss this behavior in connection to the pairing phase transition.

PACS numbers: 21.60.Jz, 25.30.Pt, 26.20.Np, 26.30.Jk

## I. INTRODUCTION

$\beta^-$ -decay of neutron-rich nuclei is one of the important subjects for r-process nucleosynthesis. In the r-process, nuclei rapidly capture neutrons and reach the neutron-rich region, until the timescale of neutron capture is comparable to that of the photodisintegration in the vicinity of the neutron shell gaps  $N=50, 82$ , and  $126$ . The  $\beta^-$ -decay becomes important mainly at this point. It increases the atomic number of neutron-rich nuclei, and eventually enables them to go on capturing neutrons again toward heavier nuclei. Therefore, the  $\beta^-$ -decay half-lives of neutron-rich nuclei determine the r-process time scale, and thus considerably influence the final abundance of elements. Likewise, the  $\beta^+$ -decay plays a decisive role in the evolution of rp-processes elements [1].

Most  $\beta^-$ -decay rates of neutron-rich nuclei relevant to the r-process have not yet been measured experimentally. Therefore, r-process calculations have to rely on a theoretical estimate of  $\beta$ -decay half-lives. Several theoretical approaches have been developed so far. One of the most widely used theoretical methods is the gross theory [2], which describes the  $\beta$ -decay rates with a sum rule approach supplemented by a statistical treatment for final states. Although it has enjoyed considerable success, it is not clear how well the shell and pairing effects for weakly bound systems are treated in the theory. Another approach is the shell model, which successfully reproduces the experimental half-lives of waiting-point nuclei at  $N=50, 82$ , and  $126$  [3, 4, 5]. However, a large-scale shell model calculation for a systematical study for heavy nuclei along the r-process path has been limited so far.

The proton-neutron quasi-particle RPA (pnQRPA) [6, 7, 8, 9, 10, 11, 12, 13, 14, 15, 16, 17] is suitable for bridging the gap between the two approaches. Being the microscopic approach, the pnQRPA properly takes into account the shell and pairing effects, and moreover it is ideal for a systematic study. The strength that contributes to the  $\beta^-$  decay mainly comes from a small low-energy tail of the Gamow-Teller (GT) distribution,

which is in general difficult to reproduce accurately with the pnQRPA. However, the pnQRPA approach based on the microscopic self-consistent mean-field framework has successfully reproduced the  $\beta$ -decay half-lives for neutron-rich isotopes by appropriately adjusting the proton-neutron pairing strength in the isospin  $T=0$  channel [9, 10, 11, 12].

The r-process takes place in an environment of high temperatures ( $T \sim 10^9$  K) and high neutron densities ( $\rho \geq 10^{20}$  neutrons/cm<sup>3</sup>). In this environment, a part of excited states is thermally populated, and in principle one needs a finite temperature treatment for  $\beta$ -decay calculations for r-process. Notice that the thermal effects affect especially low-lying states, which are important for the  $\beta$ -decay. The thermal effects on the  $\beta$ -decay rates has been studied with an independent particle model [18] and with the finite range droplet model (FRDM) plus gross theory [19]. The temperature dependence of electron capture rates has also been studied with large-scale shell model calculations[5] as well as with pnRPA with Skyrme interaction[20].

In this paper, we assess the thermal effects on the  $\beta$ -decay of neutron-rich nuclei using the pnQRPA approach. A similar attempt has been done in Refs. [13, 14, 21, 22], but they have used a schematic separable force for the particle-hole interaction. Some of them have neglected also the proton-neutron pairing correlation. We instead carry out our calculations based on the finite temperature Skyrme Hartree-Fock + BCS method, together with a contact force for the proton-neutron particle-particle interaction in pnQRPA.

The paper is organized as follows. In Sec. II, we summarize the theoretical method for finite-temperature QRPA. In Sec. III, we show the calculated results for the isotones with neutron magic number  $N = 82$ , which are relevant to the r-process nucleosynthesis. In Sec. IV, we give a summary of the paper.

## II. THEORETICAL METHODS

### A. Finite temperature Hartree-Fock + BCS method

In order to study  $\beta$ -decays at finite temperatures, we first construct the basis states using the finite temperature Hartree-Fock+BCS method [23, 24]. The formalism of the finite temperature Hartree-Fock + BCS method is almost the same as that at zero-temperature [25, 26, 27, 28], except for the particle number and pairing densities. At zero temperature, the single-particle occupation probability  $n_i$  is given by the BCS occupancy  $v_i^2$ . On the other hand, at finite temperatures  $\beta = 1/kT$ ,  $k$  being the Boltzmann constant, it is modified to,

$$\begin{aligned} n_i(T) &= f_i(T) + \tanh\left(\frac{\beta E_i}{2}\right) v_i^2, \\ f_i(T) &= \langle \alpha_i^\dagger \alpha_i \rangle = \frac{1}{1 + \exp(\beta E_i)}, \end{aligned} \quad (1)$$

where  $\alpha_i^\dagger$  and  $f_i(T)$  are the creation operator and the occupation probability for a quasi-particle, respectively.  $E_i = \sqrt{(\epsilon_i - \lambda)^2 + (\Delta_i)^2}$  is the quasi-particle energy, where  $\epsilon_i$  and  $\lambda$  are the single-particle energy and Fermi energy, respectively, and the pairing gap  $\Delta_i$  obeys the gap equation,

$$\Delta_i = -\frac{1}{2} \sum_{j>0} V_{i\bar{i}j\bar{j}} \frac{\Delta_j}{E_j} \tanh\left(\frac{\beta E_j}{2}\right). \quad (2)$$

Here,  $V$  is the pairing interaction and  $\bar{i}$  is the time-reversed state of  $i$ .

With the densities obtained with the single-particle occupation probabilities  $n_i$ , the self-consistent solution is sought by minimizing the free energy,

$$F = E - TS(T), \quad (3)$$

where  $E$  is the Hartree-Fock energy and  $S(T)$  is the entropy defined as,

$$S(T) = -k \sum_i f_i(T) \ln f_i(T) + (1 - f_i(T)) \ln (1 - f_i(T)). \quad (4)$$

In the calculations shown below, we use the smooth cutoff scheme for the pairing active space, following Ref. [26, 29]. That is, the quasi-particle energy and the gap equation are modified to  $E_i = \sqrt{(\epsilon_i - \lambda)^2 + (\gamma_i \Delta_i)^2}$  and

$$\Delta_i = -\frac{1}{2} \sum_{j>0} V_{i\bar{i}j\bar{j}} \frac{\Delta_j}{E_j} \tanh\left(\frac{\beta E_j}{2}\right) \gamma_i, \quad (5)$$

respectively. Here, the cutoff function is defined as [26, 29],

$$\gamma_i = \frac{1}{1 + \exp[(\epsilon_i - \lambda - \Delta E)/\mu]}, \quad (6)$$

with  $\mu = \Delta E/10$ . The variable  $\Delta E$  is determined so as to satisfy,

$$N_{act} = \sum_i \gamma_i = N_q + 1.65 N_q^{2/3}, \quad (7)$$

where  $N_q$  is the number of particle for proton ( $q=p$ ) or neutron ( $q=n$ ).

In our calculation, we employ the zero-range density dependent force,

$$V_{\text{pair}}(\mathbf{r} - \mathbf{r}') = V_q^0 \left(1 - \frac{\rho(\mathbf{r})}{\rho_0}\right) \delta(\mathbf{r} - \mathbf{r}'), \quad (8)$$

for the like-particle (proton-proton and the neutron-neutron) pairing interactions. We neglect the proton-neutron pairing for the BCS calculation, although it is taken into account in the QRPA calculation, because we are interested in neutron-rich nuclei, rather than  $N \simeq Z$  nuclei, in which the proton-neutron pairing plays a minor role. For the parameters for the pairing interaction in Eq. (8), we fix  $\rho_0$  to be  $0.16 \text{ fm}^{-3}$  and adjust the strength parameter  $V_q^0$  so as to reproduce the empirical values for the pairing gap obtained from the three-point mass difference  $\Delta^{(3)}(N+1)$  [30].

### B. Finite temperature quasi-particle random phase approximation (FT-QRPA)

Collective motions of hot stable nuclei have been studied with the finite temperature random phase approximation (FTRPA) [31, 32, 33, 34]. It was firstly developed for studying the giant dipole resonance of a hot compound nucleus formed in heavy-ion reactions. To discuss the property of hot exotic nuclei, the finite temperature quasi-particle RPA (FT-QRPA) was recently employed in Ref. [35]. The finite temperature proton-neutron QRPA has also been developed in Refs. [21, 22] for a separable interaction.

The applicability of the finite-temperature RPA has been assessed with the Lipkin-Meshkov-Glick method [36, 37, 38, 39]. These studies have shown that the finite-temperature RPA works satisfactorily well for the total strength. When the interaction is small so that the ground state is spherical, the FTRPA also yields a reasonable strength function. Because the proton-neutron coupling is usually weak (that is, the isovector interaction is not large enough to 'deform' the ground state in the isospin space), we argue that the finite-temperature pnQRPA provides a reasonable tool to discuss the thermal effects on the  $\beta$ -decay rate.

At finite temperatures, the quasi-particle states are thermally occupied according to the quasi-particle occupancy  $f_i(T)$  in Eq. (1). Therefore, the excitations involve both two-quasiparticle excitations and one-quasiparticle one-quasihole excitations, as is schematically shown in Figure 1. This can be understood as follows (see Fig. 2). At zero-temperature, the excited states corresponds to

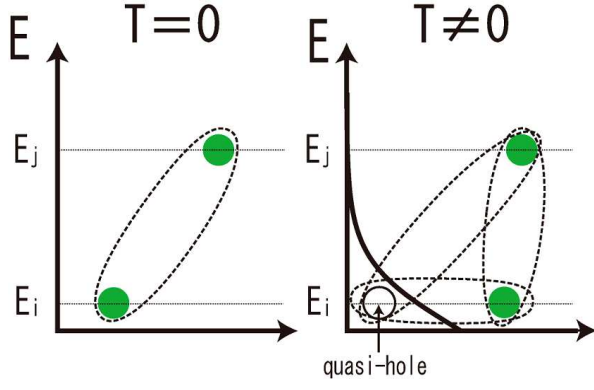


FIG. 1: (Color online) A schematic illustration for the excited states in QRPA. At zero temperature (the left panel), excited states correspond to two quasi-particle (2qp) states, while one-quasi-particle one-quasi-hole (1qp-1qh) states are also involved at finite temperatures (the right panel). The occupation probability of one quasi-particle states is given by  $f_i(T)$  in Eq. (1).

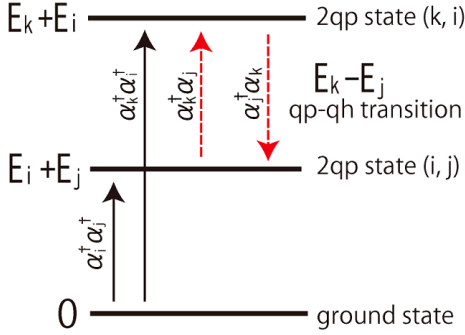


FIG. 2: (Color online) A schematic illustration for excitation scheme in finite-temperature QRPA. Transitions from the ground state corresponds to a two-quasiparticle excitation,  $\alpha^\dagger \alpha^\dagger$ , whereas the transitions among two-quasiparticle states are described by the operator  $\alpha^\dagger \alpha$ .

two-quasi-particle states built on the quasi-particle vacuum. At finite temperatures, these excited states are thermally populated. The transitions among the two-quasiparticle states are then described by the operator  $\alpha^\dagger \alpha$ , *e.g.*,

$$\alpha_k^\dagger \alpha_i^\dagger |0\rangle = \alpha_k^\dagger \alpha_j [\alpha_j^\dagger \alpha_i^\dagger |0\rangle]. \quad (9)$$

The energy change for this transition is

$$\Delta E = (E_k + E_i) - (E_i + E_j) = E_k - E_j. \quad (10)$$

The transition operator at a finite temperature thus reads [33],

$$Q^\dagger = \sum_{\alpha, \beta} P_{\alpha\beta} \alpha_\alpha^\dagger \alpha_\beta + X_{\alpha\beta} \alpha_\alpha^\dagger \alpha_\beta^\dagger - Q_{\alpha\beta} \alpha_\alpha \alpha_\beta^\dagger - Y_{\alpha\beta} \alpha_\alpha \alpha_\beta. \quad (11)$$

where  $\alpha$  and  $\beta$  run over proton and neutron levels, respectively. The first and third terms in Eq. (11) correspond to the transitions among the two-quasiparticle

states, which vanish at zero-temperature. The QRPA equation can be derived from the equation of motion,  $\langle [\delta Q, [H, Q^\dagger]] \rangle = E_{\text{QRPA}} \langle [\delta Q, Q^\dagger] \rangle$ , where  $E_{\text{QRPA}}$  is the QRPA excitation energy and  $\delta Q$  is any one-body operator. This yields,

$$\begin{pmatrix} \tilde{C} & \tilde{a} & \tilde{D} & \tilde{b} \\ \tilde{a}^T & \tilde{A} & \tilde{b}^T & \tilde{B} \\ -\tilde{D} & -\tilde{b} & -\tilde{C} & -\tilde{a} \\ -\tilde{b}^T & -\tilde{B} & -\tilde{a}^T & -\tilde{A} \end{pmatrix} \begin{pmatrix} \tilde{P} \\ \tilde{X} \\ \tilde{Q} \\ \tilde{Y} \end{pmatrix} = E_{\text{QRPA}} \begin{pmatrix} \tilde{P} \\ \tilde{X} \\ \tilde{Q} \\ \tilde{Y} \end{pmatrix} \quad (12)$$

where the elements of the matrices  $\tilde{A}, \tilde{B}, \tilde{C}, \tilde{D}, \tilde{a}$ , and  $\tilde{b}$  are given by [33],

$$\begin{aligned} \tilde{A}_{\alpha\beta\alpha'\beta'} &= \sqrt{1-f_\alpha-f_\beta} A'_{\alpha\beta\alpha'\beta'} \sqrt{1-f_{\alpha'}-f_{\beta'}} \\ &\quad + (E_\alpha + E_\beta) \delta_{\alpha\alpha'} \delta_{\beta\beta'} \\ \tilde{B}_{\alpha\beta\alpha'\beta'} &= \sqrt{1-f_\alpha-f_\beta} B_{\alpha\beta\alpha'\beta'} \sqrt{1-f_{\alpha'}-f_{\beta'}} \\ \tilde{C}_{\alpha\beta\alpha'\beta'} &= \sqrt{f_\beta-f_\alpha} C_{\alpha\beta\alpha'\beta'} \sqrt{f_{\beta'}-f_{\alpha'}} \\ &\quad + (E_\alpha - E_\beta) \delta_{\alpha\alpha'} \delta_{\beta\beta'} \\ \tilde{D}_{\alpha\beta\alpha'\beta'} &= \sqrt{f_\beta-f_\alpha} D_{\alpha\beta\alpha'\beta'} \sqrt{f_{\beta'}-f_{\alpha'}} \\ \tilde{a}_{\alpha\beta\alpha'\beta'} &= \sqrt{f_\beta-f_\alpha} a_{\alpha\beta\alpha'\beta'} \sqrt{1-f_{\alpha'}-f_{\beta'}} \\ \tilde{b}_{\alpha\beta\alpha'\beta'} &= \sqrt{f_\beta-f_\alpha} b_{\alpha\beta\alpha'\beta'} \sqrt{1-f_{\alpha'}-f_{\beta'}}, \end{aligned} \quad (13)$$

with

$$\begin{aligned} A'_{\alpha\beta\alpha'\beta'} &= V_{\alpha\beta\alpha'\beta'} (u_\alpha u_\beta u_{\alpha'} u_{\beta'} + v_\alpha v_\beta v_{\alpha'} v_{\beta'}) \\ &\quad + V_{\alpha\bar{\beta}'\bar{\alpha}'\beta} (u_\alpha v_\beta u_{\alpha'} v_{\beta'} + v_\alpha u_\beta v_{\alpha'} u_{\beta'}) \\ B_{\alpha\beta\alpha'\beta'} &= V_{\alpha\beta'\bar{\alpha}'\bar{\beta}} (u_\alpha v_\beta v_{\alpha'} u_{\beta'} + v_\alpha u_\beta u_{\alpha'} v_{\beta'}) \\ &\quad - V_{\alpha\bar{\beta}\bar{\alpha}'\beta'} (u_\alpha u_\beta v_{\alpha'} v_{\beta'} + v_\alpha v_\beta u_{\alpha'} u_{\beta'}) \\ C'_{\alpha\beta\alpha'\beta'} &= V_{\alpha\beta'\bar{\beta}\alpha'} (u_\alpha u_\beta u_{\alpha'} u_{\beta'} + v_\alpha v_\beta v_{\alpha'} v_{\beta'}) \\ &\quad - V_{\alpha\bar{\beta}\bar{\beta}'\alpha} (u_\alpha v_\beta u_{\alpha'} v_{\beta'} + v_\alpha u_\beta v_{\alpha'} u_{\beta'}) \\ D_{\alpha\beta\alpha'\beta'} &= -V_{\alpha\bar{\beta}\bar{\alpha}'\bar{\beta}'} (u_\alpha v_\beta v_{\alpha'} u_{\beta'} + v_\alpha u_\beta u_{\alpha'} v_{\beta'}) \\ &\quad + V_{\alpha\bar{\beta}'\bar{\alpha}'\beta} (u_\alpha u_\beta v_{\alpha'} v_{\beta'} + v_\alpha v_\beta u_{\alpha'} u_{\beta'}) \\ a_{\alpha\beta\alpha'\beta'} &= V_{\alpha\bar{\beta}\alpha'\beta'} (v_\alpha u_\beta v_{\alpha'} v_{\beta'} - u_\alpha v_\beta u_{\alpha'} u_{\beta'}) \\ &\quad - V_{\alpha\bar{\beta}'\beta\alpha'} (v_\alpha v_\beta v_{\alpha'} u_{\beta'} - u_\alpha u_\beta u_{\alpha'} v_{\beta'}) \\ b_{\alpha\beta\alpha'\beta'} &= V_{\bar{\alpha}\beta\alpha'\beta'} (v_\alpha u_\beta u_{\alpha'} u_{\beta'} - u_\alpha v_\beta v_{\alpha'} v_{\beta'}) \\ &\quad - V_{\alpha\beta'\bar{\beta}\bar{\alpha}'} (v_\alpha v_\beta u_{\alpha'} v_{\beta'} - u_\alpha u_\beta v_{\alpha'} u_{\beta'}). \end{aligned} \quad (14)$$

Using the solution of the QRPA equation, the strength function  $S^\pm(E)$  for the GT transition is calculated as ,

$$\begin{aligned} S^\pm(E_\nu) &= \frac{1}{1 - \exp(-\beta E_\nu)} \\ &\times \left| \sum_{\alpha > \beta} \langle \alpha | \mathcal{O}_{GT}^\pm | \beta \rangle \left( (u_\alpha u_\beta P_{\alpha\beta}^\nu + v_\alpha v_\beta Q_{\alpha\beta}^\nu) \sqrt{f_\beta - f_\alpha} \right. \right. \\ &\quad \left. \left. + (u_\alpha v_\beta X_{\alpha\beta}^\nu + v_\alpha u_\beta Y_{\alpha\beta}^\nu) \sqrt{1 - f_\beta - f_\alpha} \right) \right|^2 \\ &\times \delta(E_\alpha - E_\beta - E_\nu), \end{aligned} \quad (15)$$

where  $\mathcal{O}_{GT}^\pm = \sigma \tau^\pm$ . For  $T = 0$ , one can see that the Eqs. (12) and (15) are correctly reduced to the usual QRPA equation at zero temperature.

In our calculations, we use the  $t_0$  and  $t_3$  terms in the Skyrme force [40] as the residual interaction,

$$v(\mathbf{r}, \mathbf{r}') = - \left( \frac{t_0}{4} + \frac{t_3}{24} \rho^\alpha(\mathbf{r}) \right) (\boldsymbol{\sigma} \cdot \boldsymbol{\sigma})(\boldsymbol{\tau} \cdot \boldsymbol{\tau}) \delta(\mathbf{r} - \mathbf{r}'), \quad (16)$$

for the Gamow-Teller transition. For the particle-particle matrix elements (the proton-neutron isospin  $T=0$  pairing) in Eq. (14), we use a  $\delta$ -type interaction,

$$V_{pn}(\mathbf{r}, \mathbf{r}') = V_{pn}^0 \delta(\mathbf{r} - \mathbf{r}'). \quad (17)$$

We can regard  $V_{pn}^0$  as a free parameter as has been discussed in Ref. [9], because we do not take into account the  $T=0$  pairing in the Hartree-Fock calculation. The Gamow-Teller low-lying strengths are sensitive to the  $T=0$  pairing, and we adjust the value of  $V_{pn}^0$  to reproduce the known experimental  $\beta$  half-life at zero temperature [9, 17].

We solve the QRPA equation by diagonalizing the QRPA matrix in Eq.(12). In order to include continuum states, we discretize them with a box boundary condition with the box size of 15 fm. We include the single-particle states up to  $\epsilon = 20$  MeV, and truncate the QRPA model space at the two quasi-particle energy of  $E_{2qp} = 70$  MeV. Our pnQRPA calculation is not fully self-consistent, since we do not include all the residual interaction terms in the Skyrme functional. We thus scale the residual interaction Eq.(16) so as to reproduce the spurious translational mode (that is, the isoscalar dipole mode) at zero energy at every temperature we consider.

### III. RESULTS

#### A. Temperature dependence of GT strengths for $N=82$ Nuclei

Let us now numerically solve the pnQRPA equations and discuss the temperature dependence of the GT strengths for even-even  $N=82$  nuclei,  $^{120}\text{Sr}$ ,  $^{122}\text{Zr}$ ,  $^{124}\text{Mo}$ ,  $^{126}\text{Ru}$ ,  $^{128}\text{Pd}$ , and  $^{130}\text{Cd}$ . For this purpose, we mainly use the SLy5 force [41] for the Skyrme parameter set. We set the proton pairing strength  $V_p = -1300 \text{ MeV}\cdot\text{fm}^{-3}$  so as to reproduce the empirical pairing gap of  $^{130}\text{Cd}$ , that is,  $\Delta_p^{(3)}(Z+1) = 0.92 \text{ MeV}$ . The proton-neutron pairing strength in Eq. (17) is adjusted to  $V_{pn}^0 = -360 \text{ MeV}\cdot\text{fm}^{-3}$  so as to reproduce the experimental  $\beta$ -decay half-life of  $^{130}\text{Cd}$  (0.195 sec.) [42], and use the same value for all the other nuclei.

We find that the strength function is almost the same as that at  $T = 0$  for temperatures less than  $T = 0.2 \text{ MeV}$ , which is considered to be the standard r-process temperature at the initial condition [43]. Figure 3 shows the GT strengths at  $T = 0.0$  (the solid line) and  $T = 0.3 \text{ MeV}$  (the dashed line) for the  $^{122}\text{Zr}$ ,  $^{126}\text{Ru}$ , and  $^{130}\text{Cd}$  nuclei as a function of  $E_m^* - E_i$ , where  $E_i$  and  $E_m^*$  are the energy of the initial and final states, respectively (See Fig.4

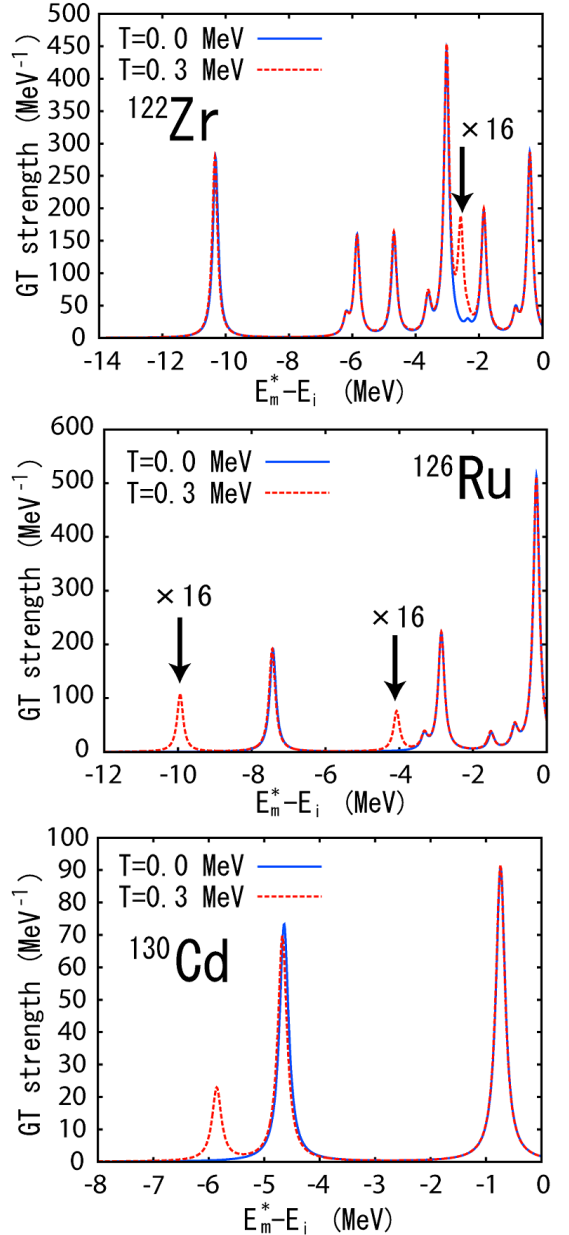


FIG. 3: (Color online) The Gamow-Teller strength functions for the  $^{122}\text{Zr}$ ,  $^{126}\text{Ru}$ , and  $^{130}\text{Cd}$  nuclei at  $T = 0.0$  (the solid line) and  $T = 0.3 \text{ MeV}$  (the dashed line). These are plotted as a function of  $E_m^* - E_i$ , where  $E_i$  and  $E_m^*$  are the energy of the initial and final states, respectively. The peaks which vanish at  $T = 0.0 \text{ MeV}$  are indicated by the arrows. For  $^{126}\text{Ru}$  and  $^{122}\text{Zr}$ , the strengths at  $T = 0.3 \text{ MeV}$  are scaled by a factor of 16.

and Eq. (21)). Those strength functions are smeared with the Lorentzian function with the width of  $0.1 \text{ MeV}$ . The strengths at  $T = 0.3 \text{ MeV}$  for  $^{126}\text{Ru}$  and  $^{122}\text{Zr}$  are multiplied by a factor of 16 for the presentation purpose. One sees that some new peaks, indicated by the arrows, appear at  $T = 0.3 \text{ MeV}$ , which originate from the transition from the excited states. Their strengths are of the

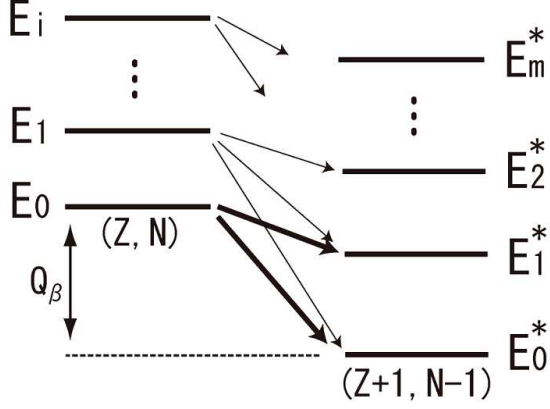


FIG. 4: A schematic illustration for the  $\beta^-$ -decay scheme at finite temperatures. The transitions at zero temperature are indicated by the thick solid arrows, while the additional transitions at finite temperatures by the thin solid arrows.

order of 0.1 on average, which are approximately of 0.1 % of the sum rule. Despite its small value, these contributions to the  $\beta$ -decay half-life cannot be neglected as we will discuss in the next section.

### B. $\beta$ -decay Half-Lives

We next calculate the  $\beta^-$ -decay half-lives. Since the contribution of the GT transition to the total  $\beta^-$ -decay rate is much larger than the Fermi transition [44], we take into account only the former. The  $\beta$ -decay half-life  $T_{1/2}$  can be calculated with the Fermi Golden rule as [9, 45],

$$\begin{aligned} \frac{1}{T_{1/2}} &= \frac{\lambda_\beta}{\ln 2} \\ &= \frac{G_F^2 g_A^2}{\ln 2 \hbar} \int_0^\infty dE_e \sum_m S^-(E_m) \rho(E_i - E_m^*, E_e), \end{aligned} \quad (18)$$

where  $\lambda_\beta$  is the  $\beta$ -decay rate.  $G_F = 1.1658 \times 10^{-11} \text{ MeV}^{-2}$  is the Fermi constant, and  $g_A = G_A/G_V$  is the ratio of the vector and pseudo vector constants, which we set 1.26. The function  $\rho(E, E_e)$  is the phase space factor for the outgoing electron and anti-neutrino given by,

$$\rho(E, E_e) = \frac{E_e \sqrt{E_e^2 - m_e^2}}{2\pi^3} (E - E_e)^2 F(Z, E_e), \quad (19)$$

where  $E_e$  is the energy of the electron and  $Z$  is the atomic number of the parent nucleus.  $F(Z, E_e)$  is the Coulomb correction factor given by [46],

$$F(Z, E_e) = 2(1+\gamma)(2k_e R_n)^{2(\gamma-1)} \left| \frac{\Gamma(\gamma + i\nu)}{\Gamma(2\gamma + 1)} \right|^2 e^{\pi\nu}, \quad (20)$$

where  $\gamma = (1 - Z^2 \alpha^2)^{1/2}$  and  $\nu = (Z \alpha E_e / p_e c)$ ,  $\alpha$  being the fine structure constant.  $k_e = p_e / \hbar$  is the electron

wave number and  $\Gamma(x)$  is the gamma function. The energy  $E_i - E_m^*$  in Eq. (19) is related to the pnQRPA energy  $E_{\text{QRPA}}$  as [9],

$$E_i - E_m^* \simeq \Delta M_{n-H} - (E_{\text{RPA}} - \lambda_n + \lambda_p), \quad (21)$$

where  $\Delta M_{n-H} = 0.78227 \text{ MeV}$  is the mass difference between a neutron and a hydrogen atom.

Figure 5 shows the  $\beta$ -decay half-lives normalized to that at zero temperature,  $T_{1/2}/T_{1/2}^0$ , as a function of temperature  $T$ . In order to check the parameter set dependence of the Skyrme functional, the figure also shows the results with the SkM\* parameter set [47]. One sees that, as the temperature increases, the  $\beta$ -decay half-life first decreases gradually for all the nuclei we study for both the parameter sets.

One can also see that the temperature dependence is the stronger for the larger atomic number. For instance, at  $T = 0.8 \text{ MeV}$ , the ratio  $T_{1/2}/T_{1/2}^0$  is around 0.2 for  $^{130}\text{Cd}$  both for the SkM\* and SLy5, while it is about 0.9 for  $^{120}\text{Sr}$ . This behavior is related with the number of the GT peaks. Figure 3 indicates that the number of GT peaks decreases gradually with the atomic number. This is due to the difference between the proton and neutron Fermi surfaces. For  $^{130}\text{Cd}$ , the number of GT peaks is only two at  $T=0$ , and the thermal effects are relatively large. On the other hand, the effects are less significant for  $^{122}\text{Zr}$  because there are already many strengths at  $T = 0.0 \text{ MeV}$ .

For  $^{122}\text{Zr}$ ,  $^{124}\text{Mo}$ , and  $^{126}\text{Ru}$ , the half-lives begin to increase at temperature around  $T = 0.6 - 0.7 \text{ MeV}$ . This is related to the temperature dependence of  $E_{\text{QRPA}}$ , which also influences the phase space factor in Eq. (19). That is, when  $E_{\text{QRPA}}$  is large, the phase space factor is also large, resulting in a large  $\beta$ -decay rate (*i.e.*, a short half-life). Since the excitation energy from the ground state,  $E_i^{\text{ex}} \equiv E_i - E_0$  and  $E_{\text{QRPA}}$  now depend on the temperature, the  $\beta$ -decay half-life may not behave in a simple way as a function of  $T$ .

A simple estimate of the thermal effect on the  $\beta$ -decay half-life can be made by disregarding the temperature dependence of  $S^-(E_m)$  in Eq. (18) except for the thermal population probability of excited levels. We approximate the population probability by the Boltzmann statistical factor,  $\exp(-E_i^{\text{ex}}/T)$ . The  $\beta$ -decay rate is then proportional to

$$e^{-(E_i - E_0)/T} \times E_e \sqrt{E_e^2 - m_e^2} (E_i - E_m^* - E_e)^2, \quad (22)$$

which has a local maximum at  $E_i = 2T + E_m^* + E_e$ . That is, the  $\beta$ -decay rate is large when the condition  $E_i^{\text{ex}} = E_i - E_0 \sim 2T + E_e - (E_0 - E_m^*)$  is satisfied. On the other hand, it is hindered considerably in the case of  $E_i^{\text{ex}} \ll 2T + E_e - (E_0 - E_m^*)$ .

In order to investigate the temperature dependence of  $E_i^{\text{ex}}$ , we plot the average pairing gaps  $\langle \Delta \rangle$  in Figure 6 and the unperturbed energy of the first excited state  $E_1^{\text{ex}} = E_1 - E_0$ , evaluated with the two-quasi-particle energy in the BCS approximation, in Figure 7. The top and

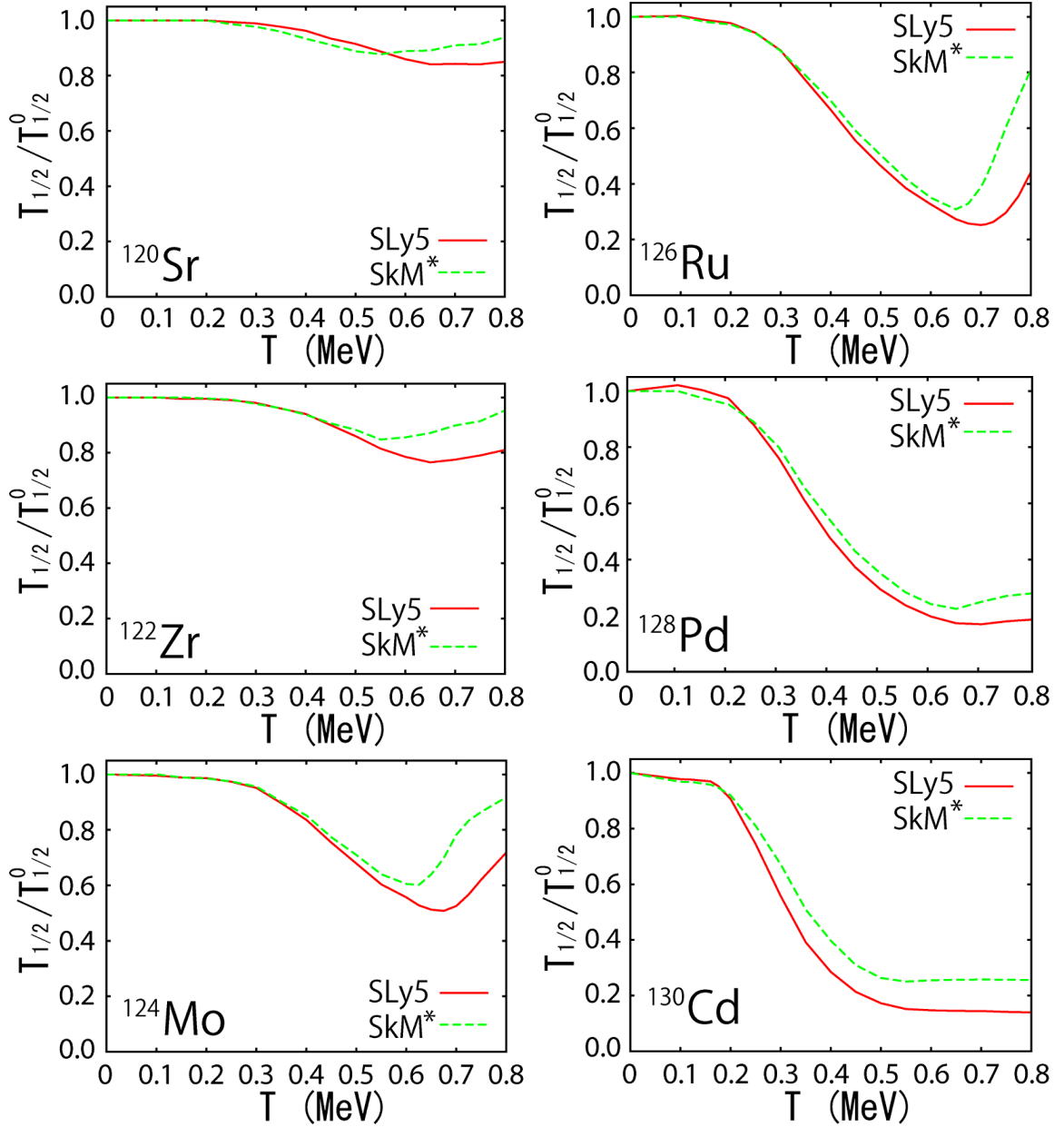


FIG. 5: (Color online) The  $\beta$ -decay half-life  $T_{1/2}$  normalized to that at zero-temperature,  $T_{1/2}^0$ . The solid and the dashed lines show the results with the SLy5 and SkM\* parameter sets, respectively.

bottom panels show the results of the SLy5 and SkM\* parameter sets, respectively. One sees that the pairing gaps begin to decrease significantly at temperatures of about  $T = 0.50 - 0.65$  MeV (*i.e.*, the pairing phase transition). Likewise, the energy of the first excited state,  $E_1^{\text{ex}}$ , also decreases rapidly at similar temperatures. For  $^{126}\text{Ru}$  and  $^{122}\text{Zr}$ , it eventually becomes less than  $2T$  at high temperatures. This should be intimately related to the increase of the  $\beta^-$ -decay half-lives for these nuclei at high temperatures. On the other hand,  $E_1^{\text{ex}}$  for  $^{130}\text{Cd}$  is much less sensitive to the temperature, as this nucleus is in the neighborhood of the double magic nucleus  $^{132}\text{Sn}$ .

As a consequence, its  $\beta$ -decay half-life monotonically decreases as a function of temperature. Note that the critical temperature for the pairing phase transition is lower for SkM\* as compared to SLy5. This fact leads to the result that the  $\beta$ -decay half-lives start increasing earlier for SkM\* compared to SLy5, as can be seen in Figure 5.

#### IV. CONCLUSION

We have assessed the thermal effects on  $\beta$ -decay half-lives with astrophysical interests for even-even isotones

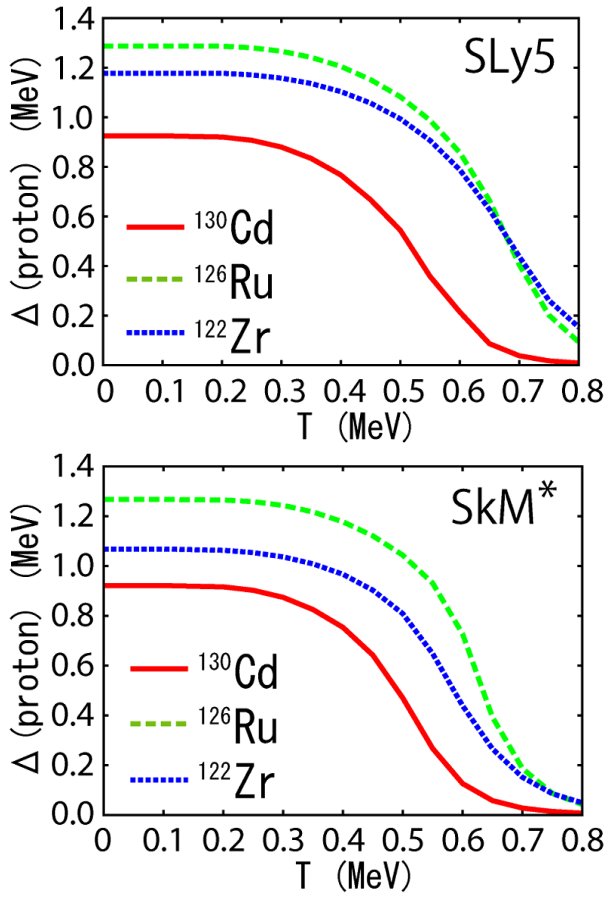


FIG. 6: (Color online) The average proton pairing gap as a function of temperature for the  $^{130}\text{Cd}$ ,  $^{126}\text{Ru}$ , and  $^{122}\text{Zr}$  nuclei. The top and bottom panels are results for the SLy5 and SkM\* parameter sets, respectively.

with the neutron magic number  $N = 82$ . For this purpose, we have adopted the finite temperature QRPA method on top of the finite temperature Skyrme-Hartree-Fock+BCS method. We have used the  $t_0$  and  $t_3$  terms of the Skyrme force for the particle-hole residual interaction, and a  $\delta$ -type interaction for the proton-neutron particle-particle channel in the QRPA formalism.

We have calculated the Gamow-Teller strengths in the temperature range from  $T = 0.0$  to  $0.8$  MeV. At finite temperatures, new peaks appear in the strength function due to the transitions from the excited states. From the calculated Gamow-Teller strengths, we have evaluated the  $\beta$ -decay half-lives. As the temperature increases, the  $\beta$ -decay half-life decreases gradually for all the nuclei which we have studied. We have also found that the temperature dependence appears more strongly for nuclei with a larger atomic number. We have argued that this is related to the number of GT peaks in the strength function, determined mainly by the difference between the proton and neutron Fermi surfaces. We have also found that the  $\beta$ -decay half-life begins to increase at

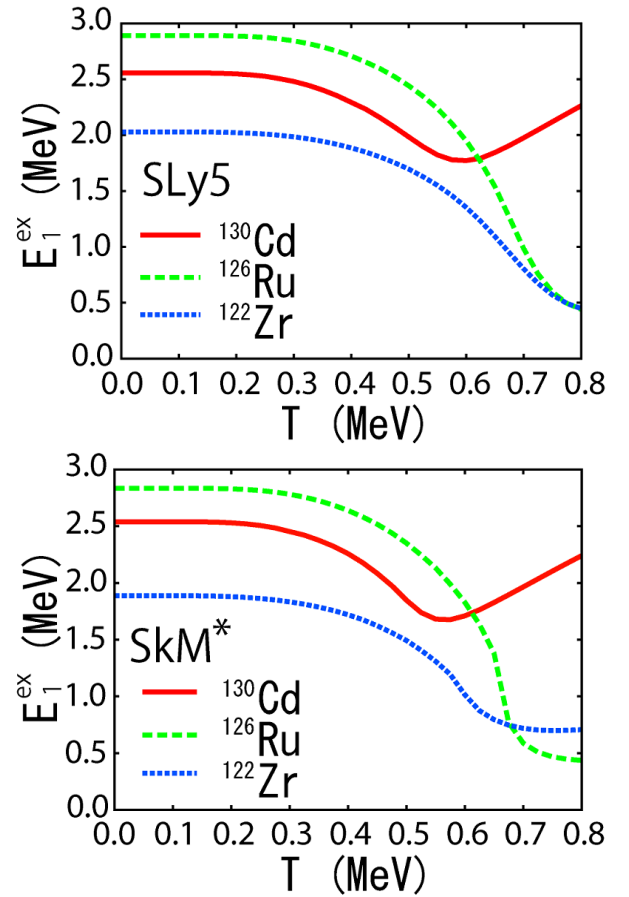


FIG. 7: (Color online) Same as Fig. 6, but for the unperturbed energy of the first excited state, estimated in the BCS approximation.

$T > 0.6 - 0.7$  MeV for open-shell nuclei as a consequence of a peculiar temperature dependence of the energy of the first excited state due to the pairing phase transition.

From our results, we conclude that the thermal effect on the  $\beta$ -decay half-life is negligible at the standard r-process temperature, which is considered to be approximately less than  $0.2$  MeV, at least for even-even  $N = 82$  isotones. It would be an interesting future problem to extend the present calculations to odd-mass nuclei, in which the energy of the first excited state is in general much smaller than that in even-even nuclei and thus a larger thermal effects may be expected.

### Acknowledgment

We thank G. Colò, T. Kajino, and H. Sagawa for useful discussions. This work was supported by the GCOE programme “Weaving Science Web beyond Particle-Matter Hierarchy” at Tohoku University, and by the Japanese Ministry of Education, Culture, Sports, Science and Technology by Grant-in-Aid for Scientific Research un-

der the program number 19740115.

- 
- [1] R.K. Wallace and S.E. Woosley, *Astrophys. J. Supp.* **45**, 389 (1981).
  - [2] K. Takahashi and M. Yamada, *Prog. Theo. Phys.* **41** (1969) 1470; T. Tachibana, M. Yamada, and Y. Yoshida, *Prog. Theor. Phys.* **84** (1990) 641.
  - [3] G. Martínez-Pinedo and K. Langanke, *Phys. Rev. Lett.* **83**, 4502 (1999).
  - [4] J.J. Cuenca-García, G. Martínez-Pinedo and K. Langanke, F.Nowacki, and I.N. Borzov, *Eur. Phys. J. A* **34**, 99 (2007).
  - [5] K. Langanke and G. Martínez-Pinedo, *Nucl. Phys. A* **673** (2000) 481.
  - [6] J. Krumlinde and P. Möller, *Nucl. Phys. A* **417**, 416 (1989).
  - [7] P. Möller and J. Randrup, *Nucl. Phys. A* **544**, 1 (1990).
  - [8] I.N. Borzov and S. Goriely, and J.M. Pearson, *Nucl Phys. A* **621**, 307 (1997).
  - [9] J.Engel *Phys. Rev. C* **60**, 014302 (1999).
  - [10] T. Niksic, T. Marketin, D. Vretenar, N. Paar, and P. Ring *Phys. Rev. C* **71**, 014308 (2005).
  - [11] T. Marketin and D. Vretenar, and P. Ring, *Phys. Rev. C* **75**, 024304 (2007).
  - [12] I.N. Borzov, *Phys. Rev. C* **67**, 025802 (2003).
  - [13] J.-U. Nabi and H.V. Klapdor-Kleingrothaus, *At. Data. Nucl. Data Tables* **88**, 237 (2004).
  - [14] J.-U. Nabi and H.V. Klapdor-Kleingrothaus, *At. Data. Nucl. Data Tables* **71**, 149 (1999).
  - [15] H. Homma, E. Bender, M. Hirsch, K. Muto, H.V. Klapdor-Kleingrothaus, and T. Oda, *Phys. Rev. C* **54**, 2972 (1996).
  - [16] A. Staudt, E. Bender, K. Muto, and H.V. Klapdor, *Z. Phys. A* **334**, 47 (1989).
  - [17] D. Cha, *Phys. Rev. C* **27**, 2269 (1983)
  - [18] G.M. Fuller, W.A. Fowler, M.J. Newman, *Astrophys. J. Supp.* **42**, 447 (1980); *Astrophys. J.* **293**, 1 (1985).
  - [19] M. A. Famiano, R. N. Boyd, T. Kajino, K. Otsuki, M. Terasawa, and G. J. Mathews *J. Phys. G : Nucl. Part. Phys.*, **35**, 025203 (2008).
  - [20] N. Paar, G. Colo, E. Khan, and D. Vretenar, [arXiv:0909.3070 \[nucl-th\]](https://arxiv.org/abs/0909.3070).
  - [21] O. Civitarese, J.G. Hirsch, F. Montani, and M. Reboiro, *Phys. Rev. C* **62**, 054318 (2000).
  - [22] O. Civitarese, M. Reboiro, *Phys. Rev. C* **63**, 034323 (2001).
  - [23] D. Vautherin *Advances in Nuclear Physics* Vol. **22**, edited by J. W. Negele and E. W. Vogt. Plenum Press, New York
  - [24] A. L. Goodman *Nucl. Phys. A* **352**, 30 (1981).
  - [25] A.L. Goodman, *Nucl. Phys. A* **352**, 30 (1981).
  - [26] C. Reiß, M. Bender, P.-G. Reinhard *Eur. Phys. J. A* **6**, 157 (1999).
  - [27] D. Vautherin and D. Brink *Phys. Rev. C* **5**, 626 (1972)
  - [28] D. Vautherin, *Phys. Rev. C* **7**, 296 (1973)
  - [29] M.Bender, K.Rutz, P.-G.Reinhard, J.A.Maruhn, *Phys. Rev. C* **60**, 034304 (1999)
  - [30] W. Satula, J. Dobaczewski, W. Nazarewicz, *Phys. Rev. Lett.* **81**, 3599 (1998).
  - [31] D. Vautherin and N. Vinh Mau *Nucl. Phys. A* **422**, 140 (1984).
  - [32] H. Sagawa and G.F. Bertsch *Phys. Lett. B* **146**, 138 (1984).
  - [33] H. M. Sommermann, *Ann. of Phys.*, **151**, 163 (1983).
  - [34] P. Ring, L.M. Robledo, J.L. Egido, and M. Faber, *Nucl. Phys. A* **419**, 261 (1984).
  - [35] E. Khan, Nguyen Van Giai, and M. Grasso *Nucl. Phys. A* **731**, 311 (2004).
  - [36] R.Rossignoli and P. Ring, *Nucl. Phys. A* **633**, 613 (1998).
  - [37] T. Hatsuda, *Nucl. Phys. A* **492**, 187 (1989).
  - [38] A.I. Vdovin and A.N. Storozhenko, *Eur. Phys. J. A* **5**, 263 (1999).
  - [39] K. Hagino and F. Minato, *Phys. Rev. C*, in press. [arXiv:0909.3345 \[nucl-th\]](https://arxiv.org/abs/0909.3345).
  - [40] Nhuyen Van Giai and H. Sagawa, *Phys. Lett.* **106B**, 379 (1981).
  - [41] E. Chabanat, P. Bonche, P. Haensel, J. Meyer, and R. Schaeffer, *Nucl. Phys. A* **635**, 231 (1998).
  - [42] K.-L. Kratz *et al.*, *Z. Phys. A* **325**, 489 (1986).
  - [43] S.E. Woosley, J.R. Wilson, G.J. Mathews, R.D. Hoffman, and B.S. Meyer, *Astrophys. J.* **433**, 229 (1994).
  - [44] K. Langanke, G. Martínez-Pinedo, *Rev. Mod. Phys.* **75**, 819 (2003).
  - [45] M.G. Bowler, *Nuclear Physics* (Pergamon Press Ltd., Headington, Hill Hall, Oxford, 1973).
  - [46] H. Behrens and W. Bühring, *Electron Radial Wave Functions and Nuclear Beta-Decay*, (Clarendon Press, Oxford, 1982).
  - [47] J.Bartel, P. Quentin, M. Brack, C. Guet, and H.-B. Hakansson, *Nucl. Phys. A* **386**, 79 (1982).